Geometries and bond energies of PHn and PHn+ (n=1–3)

K. Balasubramanian, Young Sir Chung, and William S. Glaunsinger

Citation: J. Chem. Phys. **98**, 8859 (1993); doi: 10.1063/1.464443
View online: http://dx.doi.org/10.1063/1.464443
View Table of Contents: http://jcp.aip.org/resource/1/JCPSA6/v98/i11
Published by the American Institute of Physics.

Geometries and bond energies of PH_n and PH_n^+ ($n=1$–3)

K. Balasubramanian[a)]
Department of Chemistry and Biochemistry, Arizona State University, Tempe, Arizona 85287-1604

Young Sir Chung
Science and Engineering of Materials, Center for Solid State Science, Arizona State University, Tempe, Arizona 85287-1704

William S. Glaunsinger
Department of Chemistry and Biochemistry, Arizona State University, Tempe, Arizona 85287-1604

(Received 21 December 1992; accepted 22 February 1993)

All-electron complete active space self-consistent field (CASSCF) followed by full second-order configuration interaction (SOCI) calculations which included up to 1.7 million configurations have been made on several electronic states of PH_n and PH_n^+ ($n=1$–3). A comparison is made of the results of several basis sets up to the largest set, namely, the (13*s*10*p*3*d*2 *f*1*g*/7*s*6*p*3*d*2 *f*1*g*) basis set for P and a (10*s*5*p*1*d*/8*s*4*p*1*d*) basis set for the hydrogen atom. Relativistic effective core potentials/CASSCF/multireference configuration interaction computations have also been carried out. The properties of three new excited states for PH_3 have been computed as well as the experimentally observed $X\,^1A_1$, $^3A_2'$, and $^1A_2'$ states. The calculated inversion barrier of PH_3 is 34.6 kcal/mol whereas the corresponding inversion barrier of PH_3^+ is only 2.5 kcal/mol. The bond energies of PH_n and PH_n^+ as well as adiabatic ionization energies of PH_n are computed and compared with experimental results. The core-valence and core-external correlation effects are also computed for the diatomic PH molecule.

I. INTRODUCTION

The group V hydrides such as PH_3, and AsH_3, are widely used in the microelectronics industry as source materials of the group V elements for chemical vapor deposition (CVD). Such hydrides are useful to produce quality thin films of the III–V compounds such as GaP.[1–3] These hydrides are also source materials for the corresponding dimers such as P_2, and As_2 generated through the decomposition of the corresponding hydrides.[4–10] The thermochemistry, energies and the nature of the excited states of these hydrides need to be determined to better understand the mechanism of CVD, which results in high-quality III–IV films.

The related main group (IV) hydride clusters such as SiH_n ($n=1$–4),[11] GeH_n,[11–13] and other species[14] have been studied. There are some calculations on species such as SiH_2,[15,16] GeH_2,[17,18] and NH_2 (Ref. 19) and other third-row species.[20–23] In particular, PH_3 has been studied theoretically by several investigators,[20,23,24–27] although more work has been done on the ground state of PH_3 compared to its excited states. Theoretical studies of heavier group V hydrides such as NH_n (Ref. 19) AsH_n, SbH_n, BiH_n ($n=1$–3) have also been made.[28–33]

Berkowitz *et al.*[24,34] have studied the photoionization mass spectra of PH_n ($n=1$–3). These authors have obtained the adiabatic ionization potentials of all three species. From the adiabatic ionization potentials and appearance potentials of PH_2 and PH^+, Berkowitz *et al.*[24] have predicted the bond energies $D_o(H_2P\text{–}H)$, $D_o(HP\text{–}H)$, and $D_o(P\text{–}H)$ as 82.5±0.5, 74.2±2, and 70.5±2 kcal/mol, respectively. Although the bond energies of the ground states of these species are known, there is less conclusive experimental data on the excited states of these species.

Afra and Tronc[35] have recently obtained the low-energy electron impact and high-scattering-angle energy loss spectrum of PH_3 and NH_3. These authors have observed two bands in the spectra which are attributed to the lowest energy triplet states of both NH_3 and PH_3, designated by these authors as $^3A_2''$ and $^1A_2''$. The EELS spectra of the phosphine molecule exhibited a low-intensity broad and structureless band with a maximum near 6 eV and a second narrow band at energy slightly less than 7 eV. The first band was tentatively attributed to a $^3A_2''$ excited state. The singlet–triplet energy separation was estimated as 0.89 eV from the EELS spectra. It is not clear if the valence–Rydberg mixing is important for the excited states of these molecules. The exact nature of these excited states and their geometries are not fully understood, although the ground state of this molecule appears to be well understood at the present time. Therefore, there is a need to investigate the excited states of PH_3. The only theoretical study of the excited states of PH_3 due to Müller *et al.*,[26] who have carried out mostly RHF calculations and small CI expansions (up to 1882 configurations) near the potential minima.

The objective of this investigation is to carry out accurate *ab initio* calculations on PH_n ($n=1$–3) and their positive ions using the complete active multiconfigurations self-consistent field (CASSCF) followed by the multireference singlet–doublet configuration interaction (MRSDCI) and full second-order configuration interaction (SOCI) calculations. Several large all-electron basis sets for the P atom up to (13*s*10*p*3*d*2 *f*1*g*/7*s*6*p*3*d*2 *f*1*g*) and all-electron SOCI calculations that included up to 1.7 million config-

[a)]Camille & Henry Dreyfus Teacher–Scholar. The author to whom correspondence should be addressed.

 0021-9606/93/118859-11$06.00

urations were employed. The entire inversion potential energy surfaces for the ground and an excited triplet electronic state of PH_3 were computed. The geometries are optimized and the energy separation, bond energies, and ionization potentials of PH_n ($n=1$–3) species are computed. The calculated bond energies and ionization potentials are compared with experimental results.

II. METHOD OF COMPUTATIONS

All calculations of PH_3 and PH_3^+ were made uniformly in the C_s symmetry for convenience since the codes in this work compute integrals in subgroups of D_{2h}. For the relativistic effective core potentials (RECPs) computations we used the relativistic effective core potentials for the phosphorous atom, which include the outer $3s^23p^3$ shells in the valence space replacing the rest of the electrons by relativistic effective core potentials (RECPs). A valence ($4s4p$) Gaussian basis set for P augmented with two sets of d-type polarization functions with $\alpha_{d_1} = 1.2$ and $\alpha_{d_2} = 0.3$ were employed (see Ref. 36 for further details). A more extended ($5s5p2d$) valence Gaussian basis set for the P atom was also considered. The results on PH were found to be virtually the same in the larger basis set compared to the ($4s4p2d$) basis set when used in conjunction with RECPs. In the computations done with ECPs, we employed the van Duijeneveldt ($5s1p/3s1p$) basis set for hydrogen.[37]

All-electron calculations were made on PH_n, PH_n^+ ($n=1$–3) in conjunction with large basis sets for improved accuracy. All-electron computations started with the McLean–Chandler[38] generalized Gaussian contracted-basis set of the type ($12s9p/6s5p$). The McLean–Chandler basis set is triple-zeta quality for the valence $3s$ and $3p$ orbitals of P atoms. To this basis set, three sets of six-component $3d$ type functions were added, with $\alpha_{d_1} = 0.9$, $\alpha_{d_2} = 0.3$ and $\alpha_{d_3} = 0.1$. We also augmented the s and p basis set with diffuse Rydberg $4s$ and $4p$ functions, with $\alpha_{4s}=0.02$ and $\alpha_{4p}=0.017$ suggested by Müller *et al.*[28] For accurate computations of dissociation energies of these species, $4f$ and $5g$ functions could be important. Consequently, the P basis set was extended further, with two sets of ten-component $4f$ functions, with $\alpha_{f_1} = 0.703$ $\alpha_{f_2} = 0.280$ suggested by Wu and Dunning[39] as well as one set of 15-component $5g$ functions, with $\alpha_g=0.597$. This results in a ($13s10p3d2f1g/7s6p3d2f1g$) basis set for the P atom. A comparable large basis set for the hydrogen atom was derived from the Van Duijneveldt ($10s$) primitive basis set.[37] The $10s$ basis set was contracted to a $8s$ set. This was augmented with five sets of p functions, with $\alpha_{pn} = (2.0)(0.4)^n$ for $n=0$, 1, 2, 3, 4. We also added one set of six-component d functions, with $\alpha_d=1.0$. This resulted in a ($10s5p1d/8s5p1d$) basis set for the hydrogen atom. For the diatomic PH molecule, the dissociation energy was monitored as a function of the P and H basis sets. It was found that the largest P($12s9p3d1f/6s5p3d1p$) basis set with $\alpha_f = 0.45$ yielded a D_e that is only 0.8 kcal/mol less than the $P(13s10p3d2f1g/7s6p3d2f1g)$ basis set. The six-component $3d$ functions made a difference of 0.6 kcal/mol in the D_e of the diatomic PH molecule at the second-order CI level.

Both all-electron and ECP computations were started with the complete active space self-consistent field (CASSCF) method for higher-order configuration interaction (CI) calculations. In the CASSCF method, all eight electrons in the valence space for the PH_3 molecule were distributed in all possible ways among the active orbitals which were chosen as the valence $3s$ and $3p$ orbitals of P and the $1s$ orbitals of the three H atoms. In the C_s group, the active space consisted of five a' orbitals and two a'' orbitals. All the CASSCF calculations of PH_3^+ included seven electrons in the active space. Note that excitations from the core $1s$, $2s$, and $2p$ orbitals of the P atom were not allowed in the CASSCF but these orbitals were allowed to relax for every geometry.

$^1A'$, $^3A'$, $^1A''$, and $^3A''$ states of PH_3 in the C_s symmetry for several geometries were considered. Then the states were reassigned into C_{3v} or D_{3h}, depending on whether the stationary geometry is pyramidal or planar. The entire potential energy surfaces as a function of the bond angle were considered at the CASSCF level. For each angle, the P–H bond lengths were optimized. The important regions in the potential energy surfaces were considered further for the higher-order CI (MRSDCI) computations.

The CI calculations based on the RECPs/P($4s4p2d$) CASSCF orbitals were made using the multireference singles+double configuration interaction (MRSDCI) method, which is less complete compared to the full second-order CI method considered before. In the MRSDCI method, all configurations in the CASSCF with coefficients $\geqslant 0.05$ are included. Single+double excitations were allowed from each of these reference configurations. Several electronic states of PH_3 were considered that exhibited local minima in the potential energy surfaces.

The CI computations subsequent to all-electron CASSCF computations were made using the full second-order CI (SOCI) technique. Unlike the MRSDCI, the SOCI procedure does not invoke reference configuration selection. It includes (i) all configurations in the CASSCF which is a full CI in the internal space, (ii) all configurations generated by distributing $n-1$ ($n=8$ for PH_3 and $n=7$ for PH_3^+) electrons in the internal space and an electron in the external space in all possible ways, and (iii) all configurations generated by distributing $n-2$ electrons in the internal space+2 electrons in the external space in all possible ways.

The effect of unlinked quadruple clusters is estimated through the extension of the Davidson correction to the SOCI wave function. It has been employed before by Balasubramanian and McLean[15] and is described as follows:

$$\Delta E^Q = \left(1 - \sum_{i=1}^{\text{ncsf}} C_i^2\right)[E_{\text{Ref}} - E_{(\text{SOCI})}],$$

where ncsf is the number of CASSCF configurations, C_i is the coefficient of the ith CASSCF configuration in the SOCI wave function, E_{Ref} is the energy of the wave function derived from the SOCI wave function by setting the coefficients of the first- and second-order configurations to

zero and then renormalizing, and $E_{(SOCI)}$ is the SOCI energy. The result computed including the unlinked quadruple cluster correction is referred to as the SOCI+Q result, and this is considered to be the most accurate result in a given basis set. We note that it is comforting that for most of our wave functions $\Sigma_i C_i^2$ was larger than 0.9 and thus the Q correction to the total energy was usually a few milli Hartrees. The effect of the Q correction on dissociation energies and energy separations was <0.9 kcal/mol which provides confidence to the accuracy of the SOCI expansion.

Our computations on PH_3^+ included the potential energy surfaces of the $^2A'$ state. This state gives rise to the $^2A_1$ pyramidal (but nearly planar) minimum and a higher $^2A_2''$ (D_{3h}) stationary point. We considered all-electron CASSCF/SOCI calculations, as well as ECP/CASSCF/MRSDCI of the $^2B_1$ and $^2A_1$ states of PH_2 and PH_2^+, respectively. These computations were made in the C_{2v} group, with the active space composed of three a_1 orbitals, two b_2 orbitals and one b_1 orbital. All seven electrons were included in both the CASSCF and SOCI computations. The CASSCF method considered complete distribution of all seven electrons among these active orbitals. The MRSDCI computations included all configurations in the CASSCF with coefficients $\geqslant 0.07$.

We employed the CASSCF/second-order CI methods for both all-electron and ECP calculations to compute the properties of PH and PH^+. Six outermost electrons were included in both the CASSCF and SOCI of PH, and five electrons were included for PH^+. For the diatomic PH molecule, the effect of core–valence and core–external correlation effects were also computed as follows. In the computations, which we labeled SOCI+CVCECI (core–valence–core–external configuration interaction), all possible ways of distributing 1 and 2 electrons from the core $2s^22p^6$ shells of the P atom to the five active orbitals of PH and all possible ways of distributing 1 electron from the $2s^22p^6$ core to the external space (virtual space) were considered. The dissociation energies were computed with and without the CVCECI to measure the effect of core–valence and core–external correlation effects.

All dissociation energies were computed as supermolecular CASSCF/SOCI all-electron computations to maintain consistency in the treatment of electron correlation effects. The H_2P–H bond energy was computed as a planar PH_3 supermolecule (C_{2v}) in which the dissociating hydrogen atom was placed at a 10 Å distance from P. The other two P–H bond lengths were set to the equilibrium distance (r_e) of the $^2B_1$ state of PH_2. The electronic state of the PH_3 supermolecule was chosen as $^3B_1$ in C_{2v}, since this dissociates into $PH_2(^2B_1)+H(^2S)$. Since the SOCI procedure allows all possible 0,1, and 2 electron distributions in the external space, it treats both the equilibrium geometry and the dissociated supermolecule on equal footing.

The HP–H dissociation energy was computed as a linear PH_2 supermolecule in which one P–H bond length was set to 10 Å, while the other P–H bond length was set to the equilibrium bond length of the PH diatomic molecule in its $^3\Sigma^-$ ground state. The $^4A_2$ state in C_{2v} symmetry was chosen for the supermolecule, as it yields $PH(^3\Sigma^-)+H(^2S)$ dissociated products.

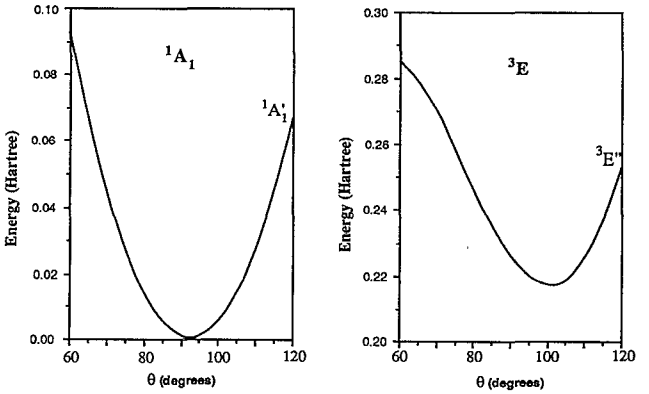

FIG. 1. Inversion potential energy surfaces for the $^1A_1$ and ^3E states of PH_3. For each θ (H–P–H angle), all three P–H bond lengths were optimized and optimized energies were plotted (see Table I for the equilibrium geometries of these and $^3A_2''$, $^1A_2''$, and $^3E''$ states).

The dissociation energy of PH was considered for the $^3\Sigma^-$ ground state in several basis sets ranging from the RECP ($4s4p2d$) basis set to an all-electron ($13s10p3d2f1g/7s6p3d2f1g$) basis set for the P atom. The $P(^4S)+H(^2S)$ dissociation limit was computed using the $^3\Sigma^-$ state computation, with the P–H bond length set to 10 Å. All CASSCF/SOCI/MRSDCI computations with RECPS and all-electron methods were carried out using Balasubramanian's[40] modified version of ALCHEMY II codes[41] to include relativistic ECPs.

III. RESULTS AND DISCUSSION

A. Geometries and energies of PH_3 and PH_3^+

1. PH_3

Figure 1 shows our computed potential energy surface of the $X\,^1A_1$ ground state of PH_3 as a function of the H–P–H bond angle (θ). For each θ, the P–H bond lengths were optimized and the optimized energy is plotted in Fig. 1. In Fig. 1, the potential energy surface of the ^3E excited state of PH_3 was also considered, which exhibits a local pyramidal minimum. However, this is not the first excited state of PH_3, as seen below. The interesting regions in the potential energy surface of PH_3 as well as excited states with planar minima were considered further.

Table I shows our all-electron results for PH_3 and PH_3^+ together with available experimental data. The angle β_e in Table I is defined as the angle between any P–H bond and the inversion plane. Consequently, β_e is 0 for planar PH_3 and its deviation from 0 measures its nonplanarity. As seen from Table I, our computed equilibrium geometry for PH_3 is in excellent agreement with experimental value of Maier and Tuner[42] (r_e within 0.0001 Å and β_e within 0.7°). Dixon *et al.*[8] have reported an experimental H–P–H bond angle of 92.1°, in agreement with our value of 92.2° for the same angle. Müller *et al.*[26] have computed r_e as 1.414 Å and β_e as 31.3° using the RHF/small CI expansion, which

TABLE I. Geometries and energies of PH_3 and PH_3^+.

Species	State	R_e(Å)[a]		β_e(deg)[a]		T_e(eV)[a]	
		Theory	Expt.	Theory	Expt.	Theory	Expt.
PH_3	$X\,^1A_1$	1.420	1.420 06[b]	33.7	33.0[b]	0	0
PH_3[c]	$^1A_1'$	1.37		0	0	1.525 (1.500)[i]	[1.37][h]
PH_3	$^3A_2''$	1.55		0		4.45 (4.42)	
PH_3	$^1A_2''$	1.68		0		5.41 (5.35)	$\Delta E(T-S)$ =0.89[d]
PH_3	^3E	1.46		28.7		5.8	
PH_3	$^3E''$	1.44		0		6.88	
PH_3	$^1E''$	1.44		0		7.31	
PH_3^+	$^2A_1$	1.38		13.5		9.66 (9.77)	9.87[e]
PH_3^+[c]	$^2A_2''$	1.39		0		9.77 (9.88)	~10.03[f]
PH_3^+	$^2A_1$	1.42		33.7		10.35	10.58[g]

[a] R_e is the P–H equilibrium bond length. β_e is the angle between the P–H bond and the inversion plane. T_e is the adiabatic energy separation.
[b] From Duncan and Mills (Ref. 35).
[c] Saddle points.
[d] Experimental triplet.
[e] Adiabatic experimental ionization energy from Berkowitz *et al.* (Ref. 24).
[f] Based on Marripu *et al.*'s (Ref. 48) inversion barrier of 0.16 eV applied to Berkowitz *et al.* (Ref. 24) ionization energy.
[g] From Maier and Turner (Ref. 42).
[h] Tentative value from Ref. 47.
[i] All numbers in parentheses are SOCI+Q results.

included up to 1882 terms for the singlet ground state. Pople and co-workers[20] obtained a θ_e=95.4° using the 631G(d) basis set for PH_3.

As seen from Fig. 1, the ^3E potential energy surface behaves similarly to the $X\,^1A_1$ surface (Fig. 1), although the well for the $X\,^1A_1$ state is much deeper compared to the ^3E surface. The r_e and θ_e values of ^3E are 1.46 Å and 97.8°. Thus the ^3E excited state shows an increase in θ compared to the $X\,^1A_1$ ground state. It is interesting to compare the potential energy curves of the ^3E state of PH_3 with AsH_3.[33] For the ^3E state of AsH_3, the H–As–H bond angle θ decreased from 92.2° for the $X\,^1A_1$ state to 86.7.

Before the excited states of PH_3 are discussed further, orbital energy diagrams are considered to gain insight into the excited states. Figure 2 shows the valence orbital energy diagrams for some of the electronic states PH_3 considered here. As seen from Fig. 2, the ground state electronic configuration of PH_3 is $1a_1^2 1e^4 2a_1^2$. The highest occupied molecular orbital (HOMO) for the pyramidal structure is the $2a_1$ orbital, while the $2e$ orbital is the lowest unoccupied molecular orbital (LUMO). The $2a_1$ orbital correlates with the $1a_2''$ orbital for the D_{3h} planar structure. Promotion of an electron from the $2a_1$ HOMO to the $2e$ LUMO yields ^3E and ^1E states in C_{3v} symmetry, of which ^3E is lower. In D_{3h} symmetry, however, the picture is more complicated, as seen from Fig. 2. The ^3E state correlates into the $^3E''$ state in the D_{3h} group with the $1a_1'^2 1e'^4 1a_2'' 2e'$ electronic configuration, since the $2a_1$ orbital correlates into $1a_2''$ while the $2e$ orbital becomes $2e'$ in D_{3h}. The reversal of $2a_1'$ and $2e'$ for the D_{3h} symmetry (see Fig. 2) produces $^3A_2''$ and $^1A_2''$ states for the planar geometry. The leading configuration of the $^3A_2''$ and $^1A_2''$ states is $1a'^2 1e'^4 1a_2'' 2a_1'$. For the planar geometry the $^3A_2''$ state would certainly be lower than $^1A_2''$ and, indeed, our computations reveal that the $^3A_2''$ state with the planar geometry is considerably lower than both ^3E (C_{3v}) and $^3E''$ (D_{3h}). It is noteworthy that Müller *et al.*[26] have also studied the dissociation pathway for the $^3A_2''$ state of PH_3 to yield $PH_2(^2B_1)+H(^2S)$.

Arfa and Tronc[33] have observed the excited states of PH_3 and NH_3 using low-energy electron impact and high scattering angle energy loss spectroscopy. The excited states of these species are quite interesting due to the possibility of valence–Rydberg mixing and the diffuse character of the Rydberg terminating orbital. Humphries, Walsh, and Warsop[44] have obtained the uv-absorption spectra of PH_3, but unfortunately the spectrum was structureless, with a band at 55 700 cm^{-1} attributed to a transition from the ground state to a singlet excited state.

The electron energy loss spectrum (EELS) of PH_3 obtained by Arfa and Tronc[33] under two conditions (at incident energy E_i=50 eV and scattering angle θ=0, and at E_i=20 eV and θ=5°) shows an interesting trend. The E_i =50 eV spectrum exhibits a single peak near 6.9 eV. The 20 eV spectrum shows more interesting features and is reminiscent of the one obtained by Robin[45] at 100 eV. The excited state in question is a $^1A_2''$ state. A vibrational progression was observed by Arfa and Tronc[33] between 8 and 9 eV that was attributed to the excitation of P. Subsequently a complex set of vibrational bands were found to converge to the ionization limit (10.58 eV). The 20 eV spectrum exhibits an interesting feature in the ~6 eV region that is tentatively attributed to the triplet counterpart of the $^1A_2''$ state. From the maxima of the two peaks, Arfa

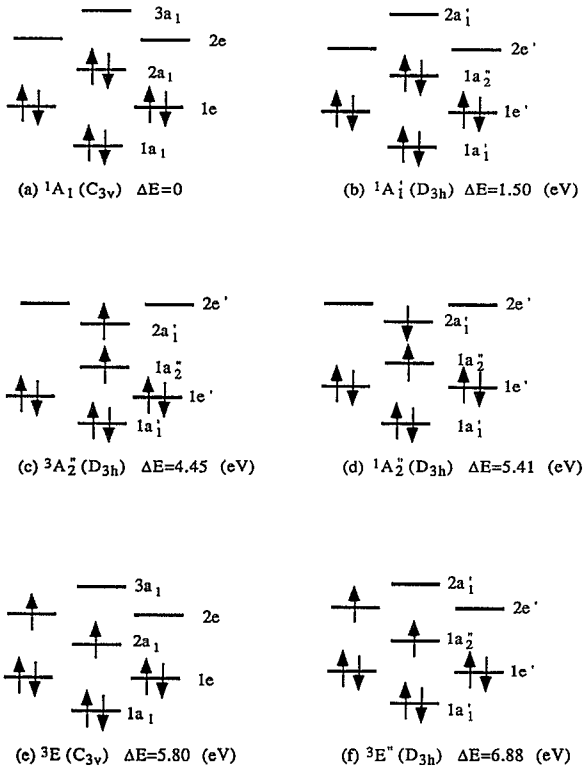

FIG. 2. Valence orbital energy diagrams for the various electronic states of PH_3.

and Tronc deduced the singlet–triplet energy separation of PH_3 as $\sim$0.89 eV.

As seen from our computed results in Table I, for the excited states of PH_3, $^3A_2''$ and $^1A_2''$ excited states are found with planar D_{3h} geometries. Our all-electron SOCI triplet–singlet ($^3A_2''$–$^1A_2''$) energy separation is 0.96 eV. A slightly improved result of 0.93 eV is obtained at the all-electron SOCI+Q level. This value should be considered in excellent agreement with the experimental estimate of 0.89 eV. Note that there is no vibrational analysis for these observed peaks and, thus, the experimental value is only an estimate. Müller *et al.*[26] obtained a S–T splitting of 0.77 eV using the RHF method with a much smaller CI expansion. It is also interesting to note that the $^3A_2''$ state is predicted to be lower than $^1A_2''$ state, in accord with the experiment. This is anticipated in view of the fact that $^3A_2''$ and $^1A_2''$ states arise predominantly from the same electronic configuration.

Although the EELS spectrum yields a T–S splitting in agreement with our computed results, one can only deduce the vertical ionization energy and the term values of the excited states. Hence, the positions of the maxima in the EELS spectrum cannot be interpreted as the adiabatic transition energies from the $X\ ^1A_1$ ground state to the corresponding excited states. This is evident from the IP obtained by Arfa and Tronc (10.58 eV), which differs from the adiabatic ionization energy of 9.87 eV obtained by Berkowitz *et al.*[24] for PH_3. Hence, the peak at 6 and 6.9 eV, which correspond to $^3A_2''$ and $^1A_2''$ states, respectively, are relative to the vertical IP of 10.58 eV. Our computed adiabatic transition energies to $^3A_2''$ and $^1A_2''$ are 4.45 (4.42) and 5.41 (5.35) where the numbers in parentheses include unlinked quadruple cluster corrections. If the difference between the vertical and adiabatic IP are introduced as a correction to the TV energies, the transition energies from the EELS spectrum are deduced to be 5.39 and 6.18 eV, respectively for the $^3A_2''$ and $^1A_2''$ states. These values are still too high compared to the computed results. Therefore the adiabatic transition energies to the $^3A_2''$ and $^1A_2''$ states need to be obtained for PH_3 with better experiments that are targeted for such measurements. Our computed results for $^3A_2''$ is closer to Müller *et al.*[26] in that they compute the $X\ ^1A_1$–$^3A_2''$ adiabatic splitting as 4.8 eV compared to our value of 4.45 eV. The r_e for the $^3A_2''$ state (1.55 Å) obtained in this work using the all-electron SOCI method is much longer compared to the value of 1.411 Å obtained by Müller *et al.*[26] using the RHF method with a small CI of 1321 terms. However, the basis set used in this study is much larger than that of Müller *et al.* and the CI expansion is considerably bigger. We have found that higher-order electron correlation effects tend to increase the bond length. Furthermore, the participation of the 4s and 4p Rydberg orbitals is very small near the equilibrium geometry of the $^3A_2''$ state. Hence, it is difficult to comprehend how the r_e of the $^3A_2''$ state could be almost identical to the $X\ ^1A_1$ ground state.

As seen from Table I, in addition to the $^3A_2''$ and $^1A_2''$ excited states, we find a ^3E excited state is found above these two states with a pyramidal equilibrium geometry. Theoretically, this state is predicted to lie at 5.8 eV above the $X\ ^1A_1$ ground state. It is surprising that this state has not yet been observed, especially considering the fact that it has a potential well (Fig. 1). The planar structure corresponding to ^3E is $\sim$1 eV above the pyramidal structure.

The inversion barrier of PH_3, i.e., the energy required to transform the pyramidal structure (C_{3v}) to the planar (D_{3h}) saddle point structure, is calculated as 1.525 eV (or 35.2 kcal/mol) at the full SOCI level of theory. The unlinked quadruple cluster correction changes the inversion barrier to 34.6 kcal/mol. Weston[46] reports an experimental inversion barrier of 31.43 kcal/mol. The SOCI+Q value obtained in this work is almost 3.3 kcal/mol below this experimental value.

The inversion barrier for PH_3 has been studied by a few authors before, namely Ahlrichs *et al.*,[47] Marynick and Dixon,[46] and Schwerdtfeger *et al.*[25] In the most recent work, Schwerdtfeger *et al.*[25] have used the Hartree–Fock single-configuration procedure followed by the Moller–Plesset second-order perturbation (MP2) level of treatment as well as extended Hückel procedures to obtain the inversion barriers for PH_3–SbH_3. For PH_3, they used P(62111+G*) and H(9s2p/6s2p) basis sets. For BiH_3, they considered MP3, MP4, and QCI levels. At the MP2 level of theory, they compute an inversion barrier of 35.1 kcal/mol, and the corresponding Hartree–Fock value reported by those authors is 35.9 kcal/mol. The barrier height, as seen from Table II, obtained in this study using the all-electron SOCI+Q level with a much larger basis set is 34.6 kcal/mol and agrees very well with the HF/MP2 result of Schwerdtfeger *et al.* The small difference of 0.5

TABLE II. Comparison of RECP/MRSDCI ($4s4p2d$)[a]. Results with all-electron/SOCI ($5s5p2d1f$) results.

Species	State	T_e(eV) RECP	T_e(eV) All-electron
PH_3	$X\,^1A_1$	0	0
PH_3	$^1A_1'$	1.6	1.525(1.500)
PH_3	$^3A_2''$	4.43	4.45(4.42)
PH_3	$^1A_2''$	5.65	5.41(5.35)
PH_3^+	$^2A_1$	9.25	9.66(9.77)
PH_3^+	$^2A_2''$	9.56	9.77(9.88)

[a]RECP results were obtained using $5e$ RECEPs for P together with P($4s4p2d$) and H($5s1p/3s1p$) basis sets and the MRSDCI method. All-electron results were obtained using the P($13s10p2d1f/7s6p2d1f$) and H($10s5p1d/8s5p1d$) basis sets and the second-order CI method. All numbers in parentheses are SOCI+Q results.

kcal/mol is probably due to the fact that the P and H basis sets are bigger and a more sophisticated CASSCF/SOCI treatment we employed in this work.

Schwerdtfeger *et al.* stated in footnote 15 of their work that Dai and Balasubramanian[33] had assumed the geometry at the inversion barrier to be planar, which needs to be clarified. Dai and Balasubramanian considered the entire potential energy surface for the inversion motion as a function of the inversion angle for AsH_3–BiH_3. In the optimized potential energy surface along the inversion pathway, the planar geometry was found to be the saddle point. This picture is uniform for NH_3–BiH_3. Of course, Dai and Balasubramanian[33] did not consider the T-shaped C_s structure, but this was considered by Schwerdtfeger *et al.* and was found to be much higher.

The inversion barrier for all heavier group V hydrides[33] was shown to be larger than PH_3. In particular, the inversion barrier for BiH_3 was found to be unusually high by Dai and Balasubramanian, who attributed this to the relativistic mass-velocity contraction of the $6s$ orbital and Schwerdtfeger *et al.*[25] confirmed this subsequently. Although Dai and Balasubramanian did not do the corresponding nonrelativistic computations, they had ample evidence from the Mulliken populations that the larger inversion barrier in the case of BiH_3 is due to the relativistic mass-velocity effect. Consider the Mulliken population of the $X\,^1A_1$ state at the pyramidal geometry and the $^1A_1'D_{3h}$ saddle point for these tri-hydrides. The transformation from pyramidal to the planar structure involves transfer of electronic density from the ns to np. It is well known that the atomic $6s$ orbital of Bi is considerably stabilized due to the relativistic mass-velocity contraction. Hence, it would take a much larger energy to promote electron density from the $6s$ to $6p$ and, thus, the higher inversion barrier in the case of BiH_3 is due to the relativistic effect.

Table II compares the results of our RECP/MRSDCI computations with a smaller P($4s4p2d$) and H($5s1p/3s1p$) basis sets and all-electron/SOCI computations made using significantly larger basis sets. First, it should be noted that the energy separations of the $^3A_2''$ and $^1A_2''$ states from the $X\,^1A_1$ state computed using the RECP method reproduce all-electron results very well. The inversion barrier height is slightly larger (1.7 kcal/mol) in the RECP/MRSDCI computation, primarily due to a smaller basis set and a lower-level of correlation treatment. The inversion barrier heights are known to become smaller at higher levels of theory. The computed adiabatic ionization energies are also too small compared to all-electron results, but are within 4% of the all-electron/SOCI results.

2. PH_3^+

The vertical ionization of the $X\,^1A_1$ ground state of PH_3 results in a $^2A_1$ open shell state for PH_3^+. The electron is removed from the highest occupied $2a_1$ orbital of PH_3. The vertical ionization potential for the process $PH_3(^1A_1) \rightarrow PH_3^+(^2A_1) + e^-$ is calculated as 10.35 eV using the RECP/MRSDCI methods compared to the experimental value of 10.58 eV obtained by Arfa and Tronc.[33] The computation of the potential energy surface of the $X\,^2A_1$ state of PH_3^+ in this work reveals that its equilibrium geometry is nearly planar. Hence, the inversion barrier is much smaller for PH_3^+ (0.11 eV), in contrast to neutral PH_3.

Marippu *et al.*[48] have obtained the high resolution photoelectron spectra of PH_3. From these spectra, they deduced the adiabatic ionization energy of PH_3 as 9.868 eV. Berkowitz *et al.* have computed the adiabatic ionization energy of $PH_3(^1A_1)$ to yield $PH_3^+(^2A_1)$ as 9.870 $\pm$0.002 eV. The very narrow error bar provided by Berkowitz *et al.* should be indicative of the high accuracy of the experimental value. At the highest all-electron SOCI and SOCI+Q levels of theory, the adiabatic IP are computed in this study to be 9.66 and 9.77 eV, respectively. The 0.1 eV increase in IP due to the unlinked quadruple cluster correction to the SOCI should be indicative of further increase in the computed IP if one were to carry out a full CI study. Consequently, the almost exact agreement obtained by Berkowitz *et al.* between their theory (9.89 eV) and experiment (9.87 eV) should be considered fortuitous considering that the best 631G**(f) basis set used by Berkowitz *et al.* is smaller than the one used in this work and that correlation effects are treated using the single-reference MP4 level of theory.

It is interesting to note that the photoionization yield curve of Berkowitz *et al.* reveals rather small vibrational gap, which is suggestive of a small inversion barrier for PH_3^+. Marippu *et al.* also find that the first vibrational gap is larger than the second one, which is indicative of a small inversion barrier for PH_3^+. This is apparently in contrast to PF_3^+.

The computed inversion barrier in this study is 0.31 eV at the RECP/MRSDCI level, and 0.11 eV at the all-electron/SOCI level which employed a much larger basis set. The computed inversion of barrier of 2.5 kcal/mol for PH_3^+ in this work is in reasonable agreement with a value of 3.7 kcal/mol reported by Marippu *et al.* using the *ab initio* CI procedure. Berkowitz *et al.* compute the inversion barrier as 2.77 kcal/mol. The HF/631–G* equilibrium r_e (P–H) for the $^2A_1$ state of PH_3^+ was computed as 1.382 Å, and the H–P–H bond angle was computed as 112.8°. These

TABLE III. Geometries and energies for the ground states of PH_2 and PH and their ions.

Species	State	R_e(Å)	θ_e(deg)	T_e(eV)
PH_2	$^2B_1$	1.418	91.6	0
PH_2^+	$^1A_1$	1.420	92.6	9.45
PH	$^3\Sigma^-$	1.425		0
PH^+	$^2\Pi$	1.427		9.87

[a]The results of PH_2 and PH_2^+ in this table were obtained using the RECP/MRSDCI treatment, while the corresponding result for PH and PH^+ were derived using the RECP/SOCI treatment.

values should be compared to the RECP/MRSDCI value of 114.7° and r_e(P–H) 1.38 Å at the same level of theory obtained in this work.

B. Geometries and energies of PH_2, PH, PH_2^+, and PH^+

Table III shows the final MRSDCI and SOCI geometries of the ground states for PH_2 and its ion and for PH and its ion, respectively. The ground state of PH_2 is of $^2B_1$ symmetry, with R_e=1.418 Å and θ_e=91.6°. These values are in excellent agreement with the experimental parameters (R_e=1.42 Å and θ_e=91.7°) obtained by Berthou *et al.*[49] The present MRSDCI result for the geometry can be compared to the previous report by Pople *et al.*[22] based on the HF/6–31G(d) model which yielded R_e=1.407 Å and θ_e=93.43°. The geometry of the ground state of the PH_2^+ positive ion ($^1A_1$) is very close to neutral PH_2, the bond length is unchanged, but the angle is slightly increased by 1°. The calculated results in this work are in full agreement with the features in the photoionization spectra of Berkowitz *et al.*[15] The first vibrational member was found to have a dominant Franck–Condon factor suggestive of a small geometry change upon ionization of PH_2 to form PH_2^+.

The ground state of PH_2 is described predominantly by the $1a_1^2 2a_1^2 1b_2^2 1b_1^1$ configuration. Thus the highest occupied orbital of PH_2 is a nonbonding b_1 orbital on P. The removal of an electron from the highest occupied $1b_1$ orbital leads to the $X\,^1A_1$ closed shell ground state of PH_2^+. The calculated adiabatic RECP/MRSDCI ionization potential of the $X\,^2B_1$ state of PH_2 is 9.45 eV. This value is too small compared to the experimental value of 9.82 eV obtained by Berkowitz and Cho.[34] However, the all-electron SOCI value obtained in this study using a much larger basis set is 9.88 eV at the SOCI level of theory, in almost exact agreement with the experimental value. As seen from Table III, the RECP/SOCI bond length of the PH $^3\Sigma^-$ ground state is 1.426 Å. Glushko *et al.*[50] note that bond length of PH (1.422 Å) is slightly larger than the P–H bond length in PH_2 (1.418 Å). The calculated results in this work are in good agreement with Ref. 50. There have also been coupled electron pair approximation (CEPA) and MRSDCI studies on PH^+.[18] The positive ion of PH shows little change in the bond length compared to the neutral PH, which is again consistent with the fact that the ionization involves removal of a nonbonding electron.

TABLE IV. Dissociation energies D_o and D_e in kcal/mol for PH_n and PH_n^+ (n=1–3).[a]

Process	Theory D_e	Theory D_o	Experiment[b]
$PH(^3\Sigma^-) \rightarrow P(^4S) + H$	71.3(72.1)	67.9(68.8)	70.1±0.5
$PH_2(^2B_1) \rightarrow PH(^3\Sigma^-) + H$	77.1(78.0)	72.2(73.1)	74.7±0.5
$PH_3(^1A_1) \rightarrow PH_2(^2B_1) + H$	84.1(84.8)	77.6(78.3)	82.5±0.5
$PH^+(^2\Pi) \rightarrow P^+(^3P) + H$	78.5(78.6)	75.1(75.2)	76.6±0.4
$PH_2^+(^1A_1) \rightarrow PH^+(^2\Pi) + H$	85.6(85.9)	80.5(80.8)	82.2±2
$PH_3^+(^2A_1) \rightarrow PH_2^+(^1A_1) + H$	83.2(84.0)	80.1(80.9)	81.5±2

[a]All theoretical results are all-electron CASSF/SOCI results except for PH. The results of PH are from the SOCI+CVCECI method and thus include the effect of core–valence and core-external correlation effects (0.23 kcal/mol). Numbers in parentheses include unlinked quadruple cluster corrections.

[b]All experimental values for the neutral PH_n are from Ref. 54. Values for the position ions were deduced from Ref. 15.

The removal of an electron from the $^3\Sigma^-$ ground state of PH leads to the $^2\Pi$ ground state of PH^+. The calculated RECP/SOCI ionization potential of PH ($^3\Sigma^-$) is 9.87 (eV). Our all-electron SOCI result with a larger basis set is 10.04 eV, while the SOCI+Q value is 10.13 eV. The experimental value reported by Berkowitz *et al.*,[24] 10.149 eV, is in excellent agreement with our computed result.

C. Bond energies and thermochemistry of PH_n and PH_n^+

Table IV shows the bond energies $D_e(H_{n-1}P–H)$ and $D_o(H_{n-1}P–H)$ computed in this work. All computations were made using the all-electron CASSCF/SOCI and CASSCF/SOCI+Q levels of theory. The zero-point corrections were taken uniformly from the work of Curtiss *et al.*[53] The theoretical zero-point energies involve an empirical scaling factor of 0.89, which is a correction factor for electron correlation effects suggested by Curtiss *et al.*[53] However, for diatomic PH, the experimental vibrational frequency for the zero-point correction was used, which is very close to the scaled theoretical zero-point correction. The basis sets employed for PH and PH^+ are P(13s10p3d2 f1g/7s6p3d2 f1g) and H(10s5p1d/8s5p1d). Hence, the results for PH and PH^+ are considered to be most accurate. The PH_3 results were obtained using slightly smaller P(13s10p2d1f/7s6p2d1f) and H(10s3p/8s3p) basis sets.

Before discussing the dissociation energies, we first consider basis-set effects. Table V shows the dissociation energies of the diatomic PH($^3\Sigma^-$) obtained using different basis sets, and the effect of core–valence and core-external correlation effects. All computations in Table V were made using the CASSCF/SOCI method. Numbers in parentheses are corrections to unlinked quadruple clusters. Only the bottom row in Table V was obtained using the RECPs for the phosphorous atom and much smaller P and H basis sets.

As shown in Table V, D_e for PH is obtained using the P(13s10p3d2 f1g/7s6p3d2 f1g) and H(10s5p1d/8s5p1d) basis sets and the SOCI+CVCECI and SOCI +CVCECI+Q values of 71.3 and 72.1 kcal/mol after correction for zero-point energy yield D_o(PH)=67.9 and 68.8

TABLE V. Dissociation energy of PH computed using different levels of theory.[a]

Basis set	Method	D_e(kcal/mol)
P(13*s*10*p*3*d*2*f*1*g*/7*s*6*p*3*d*2*f*1*g*) H(10*s*5*p*1*d*/8*s*5*p*1*d*)	CASSCF/ SOCI+CVCECI	71.3(72.1)
P(13*s*10*p*3*d*2*f*1*g*/7*s*6*p*3*d*2*f*1*g*) H(10*s*5*p*1*d*/8*s*5*p*1*d*)	CASSCF/SOCI	71.1(71.8)
P(12*s*9*p*3*d*1*f*/6*s*5*p*3*d*1*f*) H(10*s*5*p*1*d*/8*s*5*p*1*d*)	CASSCF/SOCI	70.4(71.0)
P(12*s*9*p*3*d*1*f*/6*s*5*p*3*d*1*f*) H(10*s*2*p*/8*s*2*p*)	CASSCF/SOCI	68.8(69.4)
P(12*s*9*p*2*d*1*f*/6*s*5*p*2*d*1*f*) H(10*s*2*p*/8*s*2*p*)	CASSCF/SOCI	67.0(67.3)
P(4*s*4*f*2*d*) H(5*s*1*p*/3*s*1*p*)	RECP- CASSCF/SOCI	65.0

[a]All numbers in parentheses include the effects of unlinked quadruple corrections.

kcal/mol, respectively. These values should be compared to the experimental value of 69.8±2 kcal/mol deduced by Berkowitz *et al.*[24] from the photoionization spectra. The unlinked quadruple clusters increase the D_o by almost 0.8 kcal/mol. This is suggestive of a small contribution of less than a kcal/mol in the full CI expansion compared to the SOCI+Q result. However, the relativistic and spin–orbit effects would destablize the P–H bond by the same factor. The core–valence correlation effects to the bond energies are computed as 0.2 kcal/mol (see first and second rows of Table V). Applying relativistic corrections, core–valence corrections and the full CI corrections to our SOCI+Q result, we estimate that D_e of PH should be 72.5±1 kcal/mol and thus a D_o value of 69.0±1 kcal/mol is recommended.

As also shown in Table V, there is a contribution of 1.4 kcal/mol to D_e of PH due to the Rydberg 4*s*,4*p* functions for *P* and an additional set of *f* functions and 5*g* type functions (compare the second and third rows). Hence, accurate computation (±1 kcal/mol) of dissociation energies must include at least two sets of 4*f* functions and one set of 15-component 5*g* functions, together with diffuse 4*s* and 4*p* Rydberg functions. Critical comparison of the third and fourth rows reveals that both the 3*d*-type function and several sets of *p* functions must be included for the hydrogen atom (the difference in the D_e is 1.6 kcal/mol). It is particularly noteworthy that at least three sets of 3*d*-type functions are needed for the P atom for accurate D_e computation (see fourth and fifth rows). The core–valence and core–external correlation effects increase the D_e of PH by only 0.1 kcal/mol. Finally, the RECP method with only a P(4*s*4*p*2*d*) and H(5*s*1*p*/3*s*1*p*) basis set yielded a D_e of 65.0 kcal/mol which is almost 6 kcal/mol in error compared to the best all-electron large basis set computation.

The bond energies for PH_3 and PH_3^+ in Table IV were obtained using the P(12*s*9*p*3*d*1*f*/6*s*5*p*3*d*1*f*) and H(10*s*2*p*/8*s*2*p*) basis sets. Therefore, an improvement of up to 2.7 kcal/mol in the bond energies is expected due to a somewhat smaller basis set used for PH_3. Consequently, our lower D_o value of 78.3 kcal/mol compared to an experimental value of 82.5 kcal/mol reported by Berkowitz *et al.*[24] is understandable. Furthermore, the bond energies for PH_2 and PH_2^+ obtained in this work are up to 2 kcal/mol below the experimental values of Berkowitz *et al.*, primarily due to the basis set effects discussed in detail for PH.

The photoionization spectrum of PH_3 reported by Berkowitz *et al.* show interesting trends. There are two competing processes in the photoionization of PH_3, as shown below.

$$PH_3 \rightarrow PH^+ + H_2 + e^-, \tag{1}$$

$$PH_3 \rightarrow PH_2^+ + H + e^-. \tag{2}$$

The first process is energetically more favored, as deduced from the dissociation energies of the various species, and thus occurs in the 970–1000 Å region of the spectrum (see Fig. 6 of Berkowitz *et al.*[24]). The second, less favored process occurs in the 900–940 Å region, but it is entropically more favored. The second, higher energy process could be conceivably delayed and, thus the deduced threshold for the photoionization energy could be somewhat lower. This is also reflected by the nonlinearity in the photoionization curve for the second process (Fig. 3 of Berkowitz *et al.*) compared to the first process (Fig. 6 of Berkowitz *et al.*). Consequently, there could be slight uncertainty in the estimation of the onset point for the formation of PH_2^+. Hence, the 82.5 kcal/mol D_0 for PH_3 should probably have an error bar of ±1 kcal/mol.

Berkowitz *et al.* have also considered theoretical computation of the stepwise bond energies of PH_n. They employed the Hartree–Fock method followed by MP4 level of theory. They considered four basis sets (i) 6–31G**, (ii) 6–31+G** with a set of diffuse *sp* function on P, (iii) 6–31+G**(2*d*), and (iv) 6–31G**(*f*). They assumed that the combined energy for the basis set extension from (i) to (iv) is additive. Their largest basis set 631G**(*f*) is comparable to the (12*s*9*p*2*d*1*f*/6*s*5*p*2*d*1*f*) basis set employed in this work for the P atom (cf. fourth row of Table V). Their best D_o value with this basis set for the diatomic PH is 67.6 kcal/mol. This value is comparable to our fourth row SOCI result in Table V, namely, 67 kcal/mol, and the corresponding SOCI+Q value is 67.3 kcal/mol. In a more recent work, which employed the quadratic CI(*QCI*) method together with the Gaussian-2 theory, Curtiss *et al.*[53] obtained improved total bond energies of 226.4 and 144.9 kcal/mol, respectively, for PH_3 and PH_2. In the G2 level of theory, a correction Δ is added to the previous G1 level of theory.[52] The basis set in Ref. 54, namely, 6–311+G(3*df*,2*p*), is comparable to our P(12*s*9*p*3*d*1*f*/6*s*5*p*3*d*1*f*) basis set. For the diatomic PH, we find that this basis set yields D_o~1.1 kcal/mol below experiment. It should be noted that the HF/MP4 procedure in conjunction with 631G**(*f*) basis set yielded ~3 kcal/mol below the experimental D_o for PH although the same basis set and technique yields a $D_o(H_2P–H)$ of 81.4 kcal/mol compared to the experimental value of 82.5 kcal/mol. As seen from Table V, there is a difference of 4.2 kcal/mol in the D_e of diatomic PH in going from

TABLE VI. Adiabatic ionization energies of PH_n in eV.[a]

Process	Theory	Experiment
$PH(^3\Sigma^-) \rightarrow PH^+(^2\Pi) + e$	10.04(10.13)	10.149
$PH_2(^2B_1) \rightarrow PH_2^+(^1A_1) + e$	9.88(10.00)	9.824
$PH_3(^1A_1) \rightarrow PH_3^+(^2A_1) + e$	9.66(9.77)	9.87

[a]Numbers in parentheses include unlinked quadruple clusters.

P(12*s*9*p*2*d*1*f*/6*s*5*p*2*d*1*f*), and H(10*s*2*p*/8*s*2*p*) to P(13*s*10*p*3*d*2 *f*1*g*/7*s*6*p*3*d*2 *f*1*g*) and H(10*s*5*p*1*d*/8*s*5*p*1*d*) basis sets.

As seen from Table IV, the CASSCF/SOCI+Q level of theory in conjunction with P(12*s*9*p*3*d*1*f*/6*s*5*p*3*d*1*f*) and H(10*s*2*p*/8*s*2*p*) basis sets yields 78.3 kcal/mol for $D_o(H_2P\text{–}H)$, which is almost 4 kcal/mol below the experimental value. However, a critical examination of Table V suggests an improvement of ~3 kcal/mol in moving from the third row to the first row basis set. Applying this correction, and a correction for full CI treatment, core–valence correlation effects (0.3 kcal/mol) and relativistic effects, we estimate $D_o(H_2P\text{–}H)$ to be 82 kcal/mol, which is within the experimental error bar. Hence, the experimental $D_o(H_2P\text{–}H)$ should be quite accurate despite the small uncertainty due to the two competing fragmentation processes discussed before.

The experimental dissociation energies for PH_n^+ in Table IV were deduced from the heats of formation and the thresholds for the ionization energies given in Berkowitz *et al.*'s paper, together with help from Berkowitz.[56] Our SOCI and SOCI+Q values do uniformly well for all the ions in that the computed D_o values are within 0.6–1.4 kcal/mol of the experimental values. With the exception of PH_2^+, all the PH_n^+ ions have open-shell ground electronic states.

Table VI shows the computed adiabatic ionization energies using the SOCI and SOCI+Q methods for PH_n as well as the experimental values from the work of Berkowitz *et al.* It is seen from Table VI that with the exception of PH_3, the agreement between theory and experiment is remarkably good. However, as noted before, the somewhat smaller basis set employed for PH_3 is the origin of the small difference of 0.1 eV out of 9.87 eV between our SOCI+Q result and the experimental value.

Figure 3 shows our computed SOCI+Q stepwise bond energies together with experimental values for PH_n and PH_n^+ as a function of n. First, we note that the SOCI+Q values are slightly below the experimental values. For neutral PH_n, the bond energies increase monotonically as a function of n, while for the PH_n^+ positive ions the maximum is reached for $n=2$. This is understandable in view of the closed shell $^1A_1$ ground states for PH_2^+ and PH_3.

Figure 4 shows the adiabatic theoretical (SOCI+Q) and experimental ionization energies for PH_n. It is interesting that the maximum ionization energy is for the diatomic PH. The experimental adiabatic IPs are almost the same for PH_2 and PH_3.

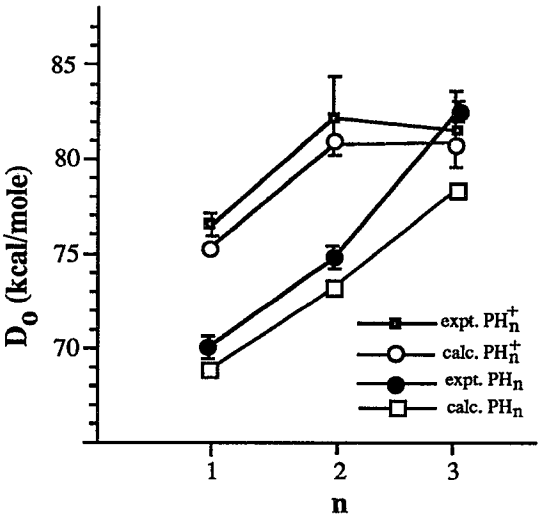

FIG. 3. Experimental and theoretical stepwise bond energies (D_o) for PH_n and PH_n^+ as a function of n.

IV. NATURE OF THE ELECTRONIC STATES OF PH_n AND PH_n^+

Here the nature of the various electronic states of PH_n and PH_n^+ are discussed through a comparison of the MRSDCI wave functions for PH_3 and PH_2 species and the SOCI wave functions for PH and Mulliken populations.

A. MRSDCI/SOCI wave functions

The leading configurations of the $X\ ^1A_1$ ground state is $1a_1^2 2a_1^2 1e^4$, with a coefficient of 0.957 in the MRSDCI wave function. The 1*e* orbital is composed of P(3*p*) orbitals and H(1*s*) orbitals. The symmetric linear combination of the H(1*s*) orbitals participates both in $1a_1$ and $2a_1$ orbitals, but to a larger extent in the $2a_1$ orbital, as the $1a_1$ orbital is predominantly composed of the P(3*s*) orbital. The ^3E excited state of PH_3 arises from the $1a_1^2 1e^4 2a_1 2e$ configuration (see also Fig. 2). The coefficient of the leading configuration for the ^3E state is 0.950. The $^2A_1$ state of PH_3^+ arises from the $1a_1^2 1e^4 2a_1$ configuration, with a coefficient of

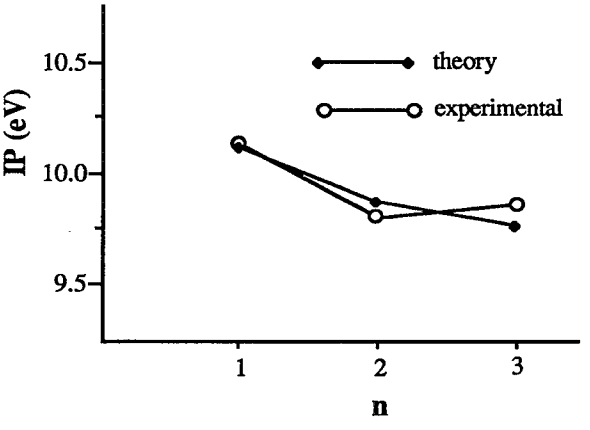

FIG. 4. Theoretical and experimental adiabatic ionization energies of PH_n (n=1–3).

TABLE VII. Mulliken population analysis of the electronic states of PH_n.

Species	State	Gross population						Overlap
		P	H	P(s)	P(p)	P(d)	H(s)	P–H
PH_3	$X\,^1A_1$	5.07	2.93	1.74	3.17	0.16	2.93	0.64
PH_3	$^1A_1'$	5.25	2.75	1.45	3.68	0.13	2.75	0.73
PH_3	^3E	4.98	2.92	1.58	3.11	0.29	2.92	
PH_3	$^3A_2''$	4.81	3.19	1.71	2.90	0.20	3.19	−0.17
PH_3	$^3E''$	5.12	2.87	1.52	3.32	0.29	2.87	
PH_3	$^1A_2''$	5.16	2.84	1.50	3.37	0.29	2.84	
PH_3^+	$^2A_1$	4.54	2.46	1.49	2.86	0.19	2.46	0.71
PH_3^+	$^2A_2''$	4.62	2.37	1.46	2.99	0.17	2.37	0.70
PH_2	$X\,^2B_1$	5.03	1.97	1.82	3.08	0.13	1.97	0.59
PH_2^+	$^1A_1$	4.30	1.70	1.71	2.37	0.22	1.70	0.65
PH	$^3\Sigma^-$	5.01	0.99	1.89	3.02	0.10	0.99	0.52
PH^+	$^2\Pi$	4.15	0.84	1.79	2.19	0.18	0.84	0.60

0.967 at the R_e and θ_e of the neutral ground state. The composition of this state is quite simple at this geometry. The planar geometry differs slightly from the pyramidal geometry in the CI composition, although the orbital compositions change. The important configuration in the MRSDCI wave function of the $^1A_1'$ saddle point is $1a_1'^2 1e'^4 1a_2''^2$. The $1e'$ orbital of the planar geometry is composed of P(p_x) and P(p_y) orbitals and H($1s$) orbitals. The $1a_2''$ orbital is composed of P(p_z). The $^3A_2''$ and $^1A_2''$ (D_{3h}) excited states of the planar PH_3 molecules arise from the $1a_1'^2 1e'^4 1a_2'' 2a_1'$ configuration. The coefficients of the leading configurations for the $^3A_2''$ and $^1A_2''$ states are 0.964 and 0.946, respectively. The leading configuration of the $^1A_2''$ state with higher energy is the same as $^3A_2''$ but it is slightly more mixed in character. The $2a_1'$ orbitals of these molecules is composed of the P(s) orbital and H($1s$) orbitals. The $1a_1'^2 1e'^4 1a_2''^1$ configuration gives rise to the $^2A_2''$ state of planar PH_3^+ ion. The coefficient of the leading configuration is 0.964, compared to 0.956 for the neutral $^1A_1'$ state of planar PH_3.

The leading valence configurations of the ground $X\,^2B_1$ and $^1A_1$ states of PH_2 and PH_2^+ are $1a_1^2 1b_2^2 2a_1^2 1b_1^1$ and $1a_1^2 1b_2^2 2a_1^2$, respectively. The coefficients of these two configurations are 0.958 and 0.953 in the MRSDCI wave function. The second and third configurations are also found to be somewhat important for both PH_2 and PH_2^+. The $^3\Sigma^-$ and ^2P ground states of PH and PH^+ ion arise from the $1\sigma^2 2\sigma^2 1\pi^2$ and $1\sigma^2 2\sigma^2 1\pi^1$ configurations, whose coefficients are 0.961 and 0.959, respectively, in the MRSDCI wave functions.

B. Mulliken population analysis

Table VII shows the gross and overlap Mulliken populations of the various electronic states of PH_n ($n=1,2,3$) and their ions. The Mulliken populations can not be used in an absolute sense since they are basis set dependent. Nevertheless, they provide qualitative insight into the charge distributions and the nature of the bonding. As seen from Table VII, the phosphorous (P) population of the $X\,^1A_1$ ground state is 5.07, which is divided into $s^{1.74}p^{3.17}d^{0.16}$. It is interesting that the polarization effect is substantial for PH_3. In comparing the Mulliken population of the (D_{3h}) $^1A_1'$ transition state to the C_{3v} pyramidal ground state, we note that the formation of the planar saddle point involves transfer of almost 0.3 electronic population from the $3s$ to the $3p$ orbital. In addition, the hydrogen population is also reduced for the planar structure compared to the C_{3v} structure. For PH_3^+ in its $^2A_1$ electronic state, the gross P population is 4.54 (H population is 2.46). This suggests that about 50% of the positive charge resides on the P atom in PH_3^+ while the rest of the charge is equitably distributed on the three hydrogen atoms. This implies that there is considerable charge redistribution upon ionization of PH_3 in its $X\,^1A_1$ ground state. In this sense, PH_3 is different from PH_2 or PH for which positive charges are predominantly on the phosphorous atom in the positive ions. Hence, the large charge redistribution for the PH_3^+ ion leads to considerable change in the geometry for the ion compared to the neutral molecule. This is the main reason for the geometry change to a planar form from the pyramidal form upon ionization of PH_3.

The individual orbital populations of PH_3^+ suggest that the ionization takes place from an orbital which involves both the $3s$ and $3p$ orbitals, since the overall population is $s^{1.49}p^{2.86}d^{0.19}$. There is very little change in the $3d$ polarization upon ionization, indicating that the polarization effects are comparable for the neutral and ionic forms.

This overall nature of the bonding and composition of the individual orbitals of PH_3 are reminiscent of AsH_3 (Ref. 33) and in contrast with NH_3. For NH_3, a bond angle of 106°47′ suggests an sp^3 hybridization, while individual Mulliken populations of the $X\,^1A_1$ state of PH_3 are $s^{1.74}p^{3.17}$. The $X\,^1A_1$ state of PH_3 shows almost the same Mulliken population compared with that of AsH_3, which is $s^{1.72}p^{3.19}$. Thus P–H bonds are made of mostly P($3p$) and H($1s$) orbitals. This explains why the bond angle in NH_3 is closer to the tetrahedral bond angle, while for PH_3, AsH_3, and other heavier analogs the H–M–H bond angles are closer to 92°. Furthermore, the smaller $3s$ participation is noted in the $2a_1$ orbital of PH_3, while the corresponding orbital of NH_3 is known to be a significant mixture of N($2s$), N($2p_z$), and [$H_1(1s)+H_2(1s)+H_3(1s)$].

As seen from Table VII, the phosphorous (P) population of PH_2 in the $X\,^2B_1$ state is 5.03, which spits into $s^{1.82}p^{3.08}d^{0.13}$. For PH_2^+ in its $^1A_1$ electronic state, the gross P population of 4.30 (H population is 1.70) suggests that most of the positive charge is predominantly on the phosphorous atom. This implies that the charge redistribution upon ionization of PH_2 in the $X\,^2B_1$ ground state is quite small. In this sense, PH_2 is different from the case of PH_3. The small charge redistribution for the PH_2^+ ion suggests a negligible change in the geometry for the ion compared to the neutral molecule. The Mulliken populations of PH and PH^+ species show a behavior similar to that of PH_2.

V. CONCLUSION

In this investigation, we carried out complete active space multiconfiguration self-consistent field (CASSCF) followed by second-order CI+Q calculations for the electronic states of PH_n and PH_n^+. Both all-electron and RECP methods were employed. The all-electron method employed up to P(13s10p3d2 f1g/7s6p3d2 f1g) and H(10s5p1d/8s5p1d) basis sets. We computed both the ground and excited states of PH_3. Our computed bond energies for PH_n and PH_n^+ were found to be in good agreement with the experimental values. For PH_3, we computed the properties of $^3A_2''$ and $^1A_2''$ excited states with D_{3h} planar equilibrium geometries and compared our triplet–singlet splitting to the EELS spectra. We also computed the properties of another excited ^3E state with pyramidal equilibrium geometry that is higher than the $^3A_2''$ and $^1A_2''$ planar states. The ^3E state is yet to be observed experimentally. Our computed inversion barrier was found to be in good agreement with previous theories, but differs from a past experimental value. This work provides the basis for more extensive calculations to understand the interactions of these species with surfaces.

ACKNOWLEDGMENTS

This research was supported in part by the United States National Science Foundation under Grant No. CHE9280499 and Motorola Inc. under Grant No. 89-1064. Y.S.C. is a recipient of a Motorola University Partnership in Research Fellowship. The authors thank Dr. D. Dai, Dr. J. Berkowitz, and Dr. L. Curtiss for helpful discussions.

[1] J. Berkowitz, J. Chem. Phys. **89**, 7065 (1988).
[2] M. B. Parish, J. Elec. Chem. Soc. **127**, 2729 (1980).
[3] B. A. Joyce, Rep. Prog. Phys. **48**, 1637 (1985).
[4] P. Bollmark and B. Lindgren, Chem. Phys. Lett. **1**, 13 (1968).
[5] N. Basco and K. K. Yee, Spectrosc. Lett. **1**, 13 (1968).
[6] P. Bollmark and B. Lindgren, Phys. Soc. **10**, 325 (1984).
[7] R. N. Dixon and H. M. Lamberton, J. Mol. Spectrosc. **25**, 12 (1968).
[8] R. N. Dixon, G. Duxbury, and H. M. Lamberton, Chem. Commun. Chem. Soc. (London) **460** (1966).
[9] B. Lindgren, Phys. Sci. **12**, 164 (1975).
[10] B. Lindgren and Ch. Nilsson, J. Mol. Spectrosc. **55**, 407 (1975).
[11] J. Berkowitz, J. P. Greene, H. Cho, and B. Ruščić, J. Chem. Phys. **86**, 1235 (1987).
[12] A. M. R. P. Bopegedera, C. R. Brazier, and P. Bernath, Chem. Phys. Lett. **162**, 301 (1989).
[13] B. Ruščić, M. Schwarz, and J. Berkowitz, J. Chem. Phys. **92**, 1865 (1990).
[14] G. T. Gibson, J. P. Greene, and J. Berkowitz, J. Chem. Phys. **85**, 4815 (1986).
[15] K. Balasubramanian and A. D. McLean, J. Chem. Phys. **85**, 5117 (1986).
[16] M. Colvin, R. S. Grev, H. F. Schaefer, III, and J. Bicerano, Chem. Phys. Lett. **99**, 399 (1983).
[17] K. Balasubramanian, J. Chem. Phys. **89**, 5731 (1988).
[18] P. J. Bruna and S. D. Peyerimhoff, Bull. Soc. Chim. (Belgium) **92**, 525 (1983); P. J. Bruna, G. Hirsch, S. D. Peyerimhoff, and R. J. Buenker, Mol. Phys. **42**, 875 (1981); P. Rosmus and W. Meyer, J. Chem. Phys. **66**, 13 (1977).
[19] S. J. Gibson, J. P. Greene, and J. Berkowitz, J. Chem. Phys. **83**, 4319 (1985).
[20] J. A. Pople, B. T. Luke, M. J. Frisch, and J. S. Binkley, J. Phys. Chem. **89**, 2198 (1985).
[21] L. A. Curtiss and J. A. Popole, Chem. Phys. Lett. **144**, 38 (1988).
[22] J. A. Pople and L. A. Curtiss, J. Phys. Chem. **91**, 3637 (1987).
[23] L. A. Curtiss and J. A. Pople, J. Phys. Chem. **92**, 894 (1987).
[24] J. Berkowitz, L. A. Curtiss, S. T. Gibson, J. P. Greene, G. L. Hilhouse, and J. A. Pople, J. Chem. Phys. **84**, 375 (1986).
[25] P. Schwerdtfeger, L. Laakkonen, and P. Pyykkö, J. Chem. Phys. **96**, 6807 (1992).
[26] J. Müller, H. Ågren, and S. Canuto, J. Chem. Phys. **76**, 5060 (1982).
[27] S.-X. Xiao, W. C. Trogler, D. E. Ellis, and Z. Benkovitch-Yellin, J. Am. Chem. Soc. **105**, 7033 (1983).
[28] K. Balasubramanian, J. Chem. Phys. **91**, 2443 (1989).
[29] K. Balasubramanian and V. Nannegari, J. Mol. Spectrosc. **138**, 482 (1989).
[30] K. Balasubramanian, N. Tanpipat, and J. E. Bloor, J. Mol. Spectrosc. **124**, 458 (1987).
[31] K. Balasubramanian, J. Mol. Spectrosc. **115**, 258 (1986).
[32] K. Balasubramanian, Chem. Rev. **89**, 1801 (1989).
[33] D. G. Dai and K. Balasubramanian, J. Chem. Phys. **93**, 1837 (1990).
[34] J. Berkowitz and H. Cho, J. Chem. Phys. **90**, 1 (1989).
[35] M. B. Arfa and M. Tronc, Chem. Phys. **155**, 143 (1991).
[36] D. W. Liao and K. Balasubramanian, J. Chem. Phys. **96**, 8938 (1992).
[37] F. B. Van Duijneveldt, IBM Res. Rep. 945 (1971).
[38] A. D. McLean and G. S. Chandler, J. Chem. Phys. **72**, 5639 (1980).
[39] D. E. Woon and T. H. Dunning, Jr., J. Chem. Phys. **98**, 1358 (1993).
[40] K. Balasubramanian, Chem. Phys. Lett. **127**, 585 (1986).
[41] The major authors of ALCHEMY II are B. Lengsfield, B. Liu, and M. Yoshimine.
[42] J. P. Maier and D. W. Turner, J. Chem. Soc. Faraday Trans. **268**, 711 (1972).
[43] R. N. Dixon, D. Duxbury, and H. M. Lamberton, Proc. R. Soc. London Ser. A **305**, 275 (1968).
[44] C. M. Humphries, A. D. Walsh, and P. A. Warsop, Discuss. Faradays Soc. **35**, 148.
[45] M. Robin, *Higher Excited States of Polyatomic Molecules*, Vol. III, (Academic, New York, 1985).
[46] R. E. Weston, J. Am. Chem. Soc. **76**, 2645 (1954).
[47] R. Ahlrichs, F. Keil, H. Lischka, W. Kutzelnigg and V. Staemmler, J. Chem. Phys. **63**, 455 (1975); R. Ahlrichs, F. Driessler, H. Lischka, V. Staemmler and W. Kutzelnigg, *ibid.* **62**, 1235 (1975); D. S. Marynick and D. A. Dixon, *ibid.* **86**, 914 (1982).
[48] R. Maripuu, I. Reineck, H. Agren, W. Nien-Zu, J. M. Rong, H. Veenhuizen, S. H. Al-Shamma, L. Karlsson, and K. Siegbahn, Mol. Phys. **48**, 1255 (1983).
[49] J. M. Berthou, B. Pascat, H. Guenebaut, and D. A. Ramsay, Can. J. Phys. **50**, 2265 (1972).
[50] V. P. Glushko, L. V. Gurvich, G. A. Bergman, I. V. Veits, V. A. Medvedev, G. A. Khachkunuzov, and V. S. Yongman, *Termidinamicheski Svoistva Individual'nikh Veschesty* (Nauka, Moscow, 1978), Vol. I, Books 1 and 2.
[51] W. C. Martin, J. Opt. Am. **49**, 1071 (1959).
[52] L. A. Curtiss, C. Jones, G. W. Trucks, K. Raghavachain and J. A. Pople, J. Chem. Phys. **93**, 2537 (1990).
[53] L. A. Curtiss, K. Raghavachari, G. W. Trucks and J. A. Pople, J. Chem. Phys. 7221 (1991).
[54] J. Berkowitz, Acc. Chem. Res. **22**, 413 (1989).
[55] J. L. Duncan and J. M. Mills, Spectro. Chem. Acta **20**, 523 (1964).
[56] J. Berkowitz (private communication).